The Impact of Vacancy Defects on CNT Interconnects: From Statistical Atomistic Study to Circuit Simulations

Jaehyun Lee[1*], Salim Berrada[1], Jie Liang[2], Toufik Sadi[1,3], Vihar P. Georgiev[1], Aida Todri-Sanial[2], Dipankar Kalita[4], Raphael Ramos[5], Hanako Okuno[4], Jean Dijon[5] and Asen Asenov[1], *Fellow IEEE*

[1]*School of Engineering, University of Glasgow, Glasgow, Scotland, UK, *Jaehyun.Lee@glasgow.ac.uk*
[2]*CNRS-LIRMM, University of Montpellier, Montpellier, France*
[3]*Department of Neuroscience and Biomedical Engineering, Aalto University, Helsinki, Finland*
[4]*CEA-INAC, University Grenoble Alpes, Grenoble, France*
[5]*CEA-LITEN, University Grenoble Alpes, Grenoble, France*

Abstract— **We have performed statistical atomistic simulations with tight-binding approach to investigate the effects of randomly distributed mono-vacancy defects in metallic single-walled carbon nanotube (SWCNT) interconnects. We also extracted defective resistances from the atomistic simulations and performed circuit-level simulations to compare the performance of interconnects with and without defects. We have found that the defects induce significant fluctuations of SWCNT resistance with a median value showing an Ohmic-like behaviour. Fortunately, the resistance depends only on the diameter of SWCNTs and not on their chirality. Moreover, our circuit simulations show that the defective resistance induces important propagation time delay ratio that should be accounted for when designing CNT interconnects.**

Keywords—interconnects, ststistical simulation, carbon nanotubes, mono-vacancy defects, defective resistance, tight-binding

I. INTRODUCTION

As the CMOS feature size has continued to shrink to the nanometer scale, the size of interconnects also has been reduced significantly. As the cross-sectional area of interconnects becomes smaller, there is a need for new materials capable of withstanding high current density (high ampacity). In addition, Cu interconnects, which are the most commonly used in the semiconductor industry, suffer from surface and grain boundary scattering effects [1, 2]. From a thermal point of view, the new material should have high thermal conductivity to prevent the temperature rise due to the self-heating.

Carbon NanoTube (CNT) interconnects have recently attracted attention as a promising technology to replace Cu interconnects in next generations of CMOS circuits thanks to their good electrical/thermal properties [3-6]. Indeed, recent experimental studies have shown that CNTs have a large ampacity - 100 times greater than that of Cu - and show a strong resistance to electro-migration due to its strong C-C bonding [7].

Despite these outstanding properties, experimental results indicate that defects could degrade the electrical properties of perfect CNTs. Indeed, a resonant transmission between defects has been observed experimentally in CNTs and has been attributed to their large phase relaxation length λ_{phase} (typically larger than that of 3-D materials) [8]. Nevertheless, there are very few theoretical studies to assess the corresponding degradation of electrical properties. In this work, we have investigated the electrical performance of metallic single-walled (SW) CNTs with mono-vacancy defects through a statistical approach and performed relevant circuit simulations.

II. SIMULATION METHOD

In this work, we have used the tight-binding (TB) – Non-Equilibrium Green's Function (NEGF) framework implemented in the Atomistix ToolKit (ATK) [9]. We have adopted the extended TB approach – which includes the third nearest neighbour hopping – to describe the Hamiltonian of CNTs [10]. All transport calculations are performed within the ballistic approximation.

Fig. 1 shows the geometric configuration of the SWCNT(24,0) interconnect with two semi-infinite electrodes. We assume that the mono-vacancy defects are randomly distributed only in the central CNT region. For the statistical study, we have used 80 samples for each case. The length of the central region (L_{ch}) ranges from 20 to 85 nm. In the case of SWCNT(24,0) with $L_{ch} = 85$ nm, the number of carbon atoms is 19,200.
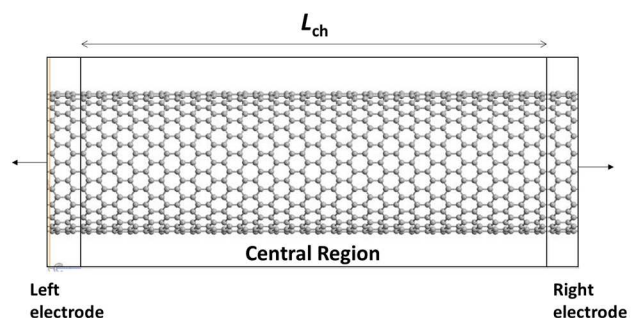

Fig. 1. Geometry of a single CNT(24,0) interconnect configuration with two semi-infinite electrodes.

We have considered the driver-interconnect-load system as shown in Fig. 2 for the circuit-level simulations. We used the specifications of the 45 nm CMOS technology node for the values of the resistances and capacitances of the driver (R_d, C_d) and receiver (R_r, C_r) which are equal to 24 kΩ and 450 aF respectively. The interconnect resistance (R_w) consists of a ballistic resistance (R_{bal}), a phonon resistance (R_{ph}), and a defective resistance (R_{def}), which is assumed to be independent of the two other resistances. The phonon scattering effects can be described by the mean free path approximation. The interconnect resistance can be written as:

$$R_w = R_{bal} + R_{ph} + R_{def}$$
$$= R_{bal} + R_{bal}\frac{L}{\lambda} + R_{def} , \qquad (1)$$

where L and λ are the interconnect length and a mean free path of the CNT, respectively [7]. Here, we assume that λ does not depend on the defects. Interconnect (C_w) and load capacitances (C_{load}) are set to 30 aF/μm and 10 fF, respectively.

We also investigated the propagation time delay (τ) ratio influenced by the defects. The propagation time delay ratio is defined as follow:

$$\tau \text{ ratio} = \tau_{perfect\ CNT} / \tau_{defectivive\ CNT}. \qquad (2)$$

III. SIMULATION RESULTS

Fig. 3 depicts the dependence of the resistance on the number of mono-vacancy defects (N_{def}) for a zigzag SWCNT(24,0) and an armchair SWCNT(14,14) having respectively 18.8 and 19.0 Å diameters. One dot indicates the result for each sample, and the red line is their median value. This figure shows that for both CNTs, the resistance value fluctuates greatly for a given number of mono-vacancy defects depending on their random spatial distribution. Moreover, we have found that the variation range increases as the number of defects increases. We attribute this resistance fluctuation to the aforementioned resonance transmission between defects. However, even for these large variation ranges, the median values have a near-linear dependence on the number of defects, exhibiting an Ohmic-like behaviour. From this figure, a relationship between N_{def} and R_{def} can be found as follows:

$$R_{def} \approx 6720 \times N_{def}. \ (\Omega) \qquad (3)$$

Fig. 4 illustrates the dependence of the resistance on L_{ch} with 6 mono-vacancy defects. Note that the median values (49.5$\pm$4.8 kΩ) do not change much with L_{ch}. This result is an important proof that this statistical study is justified by showing that it is reasonable to calculate defective resistance considering the interaction between defects on CNT interconnects shorter than their λ_{phase}. Generally, λ_{phase} has a value of a few microns and $\lambda_{phase} > \lambda$.
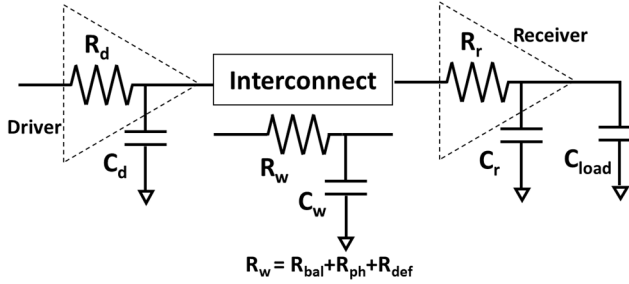

Fig. 2. Geometry of a single CNT(24,0) interconnect configuration with two semi-infinite electrodes.
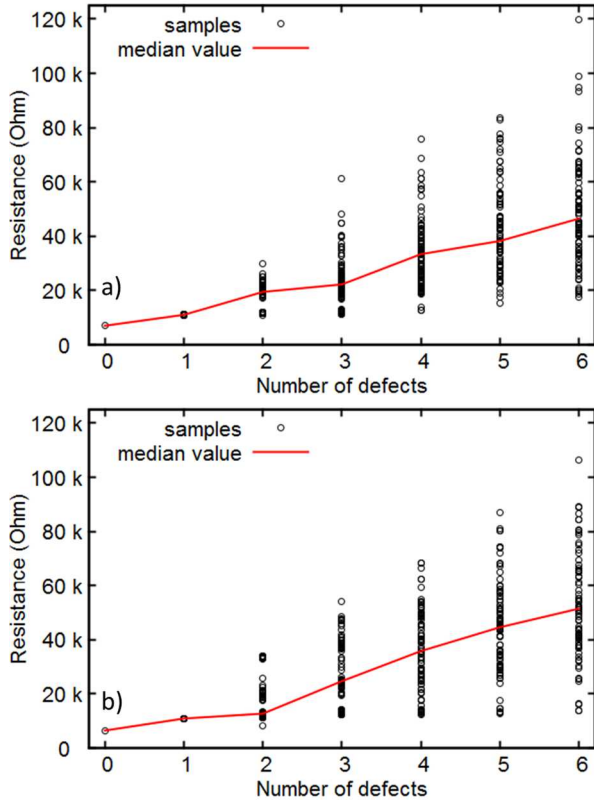

Fig. 3 Dependence of the resistance on the number of mono-vacancy defects, for a) a CNT(24,0) and b) a CNT(14,14) at 300 K. CNTs with zero defect indicate the perfect CNTs. 80 samples were used. L_{ch} is set to about 42 nm.
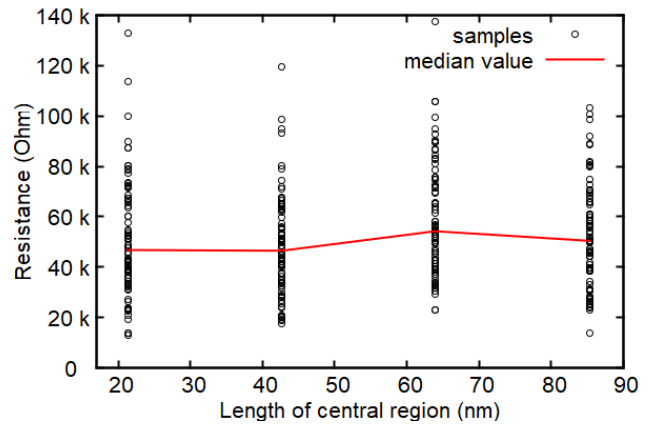

Fig. 4 Dependence on L_{ch} for a CNT(24,0) with 6 mono-vacancy defects at 300 K. 80 samples were used.
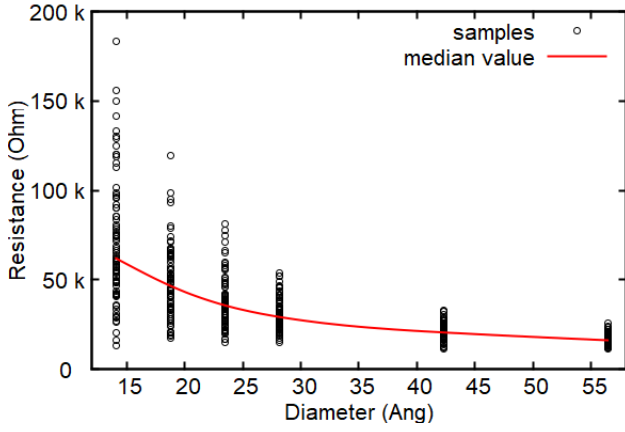
Fig. 5 Dependence of the resistance on the diameter of the zigzag SWCNT with 6 mono-vacancy defects at 300 K. 80 samples were used. L_{ch} is set to 42.6 nm.
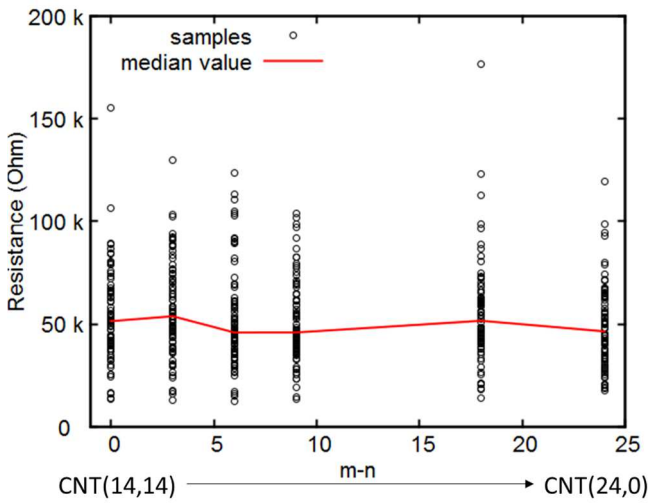

Fig 6. Dependence of the resistance on the chirality of SWCNT(m, n) with 6 mono-vacancy defects at 300 K. 80 samples were used. All CNTs have similar diameters. L_{ch} is set to close to 42 nm for fair comparison.

The dependence of the resistance on the diameter of the metallic zigzag SWCNTs (D_{CNT}) with 6 mono-vacancy defects is shown in Fig. 5; we considered SWCNT(18,0), SWCNT(24,0), SWCNT(30,0), SWCNT(36,0), SWCNT(54.0), and SWCNT(72,0) with the same L_{ch} (~ 42.6 nm) and diameters of 14.1, 18.8, 23.5, 28.2, 42.3 and 56.4 Å, respectively. It is noteworthy that the resistance decreases as the diameter increases. Moreover, the variation range decreases sharply. Because the number of carbon atoms forming the unit cell increases as the diameter increases, the probability of the six mono-vacancy defects altering the electrical performance of the SWCNT is lower for equal length.

We have found a very interesting relationship between the median values of R_{def} with 6 mono-vacancy defects and the diameter of SWCNT from Fig. 5;

$$R_{def}(6 \text{ defects}) = 1.6 \times 10^6 \times \left(D_{CNT}(\text{Å})\right)^{-1.27} \ (\Omega). \quad (4)$$
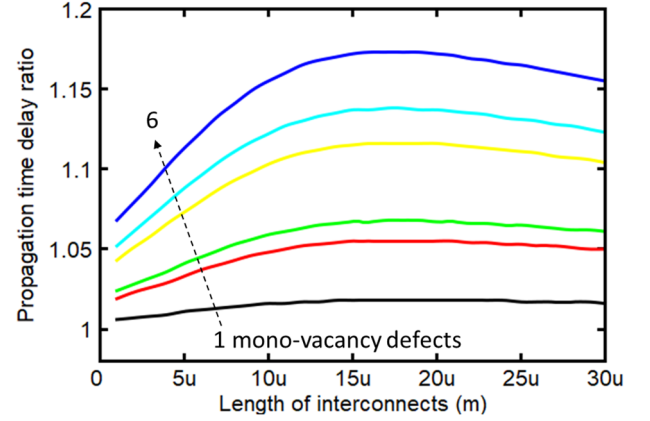

Fig. 7 The dependence of the propagation time delay ratio on the SWCNT(24,0) interconnect length obtained from the circuit simulations at 300 K..

If D_{CNT} increases to 33 nm, R_{def} with 6 mono-vacancy defects decreases to 1 kΩ.

The dependence on the chirality of SWCNT(m, n) structures with 6 mono-vacancy defects is shown in Fig. 6. We have considered only the metallic CNTs with similar diameters of SWCNT(24,0) (~18.8 Å). Our simulation results show that there is no dependence on the chirality, and the resistance for SWCNTs with a 18.8 Å diameter and 6 mono-vacancy defects is 49.2 ± 4.6 kΩ. Given the difficulty of chirality control in experiments, the fact that there is no dependence on the chirality and only dependence on the diameter is good news in terms of the CNT interconnect variability.

Based on the result that the resistance is not correlated with the chirality of SWCNT, we have obtained a general equation that can describe R_{def} from Eqs. 3 and 4;

$$R_{def}\left(N_{def}, D_{CNT}\right) = 2.67 \times 10^5 \times N_{def} \times (D_{CNT})^{-1.27}(\Omega). \quad (5)$$

Fig. 7 shows the dependence of the propagation time delay ratio for a SWCNT(24,0) as a function of the number of mono-vacancy defects. We used Eq. 5 for the values of R_{def} in the circuit-level simulation. We note that the maximum τ ratios are observed when L = 15 μm, regardless of the number of mono-vacancy defects. To understand this result, we derived the following analytical equation from the Elmore formula:

$$\tau \text{ ratio} = 1 + 0.69R_{def}(C_d + C_r + C_{load} + C_w)/\tau_p, \quad (6)$$

where τ_p is the propagation time delay for a perfect SWCNT interconnect including phonon scattering effects. Since C_w increases as L increases, τ ratio also increases. However, increasing L increases also phonon scattering (see Eq. 1) – and consequently τ_p – which becomes dominant compared to defect scattering. Thus, an inflection point of τ ratio is reached for a high enough value of L, which is independent of the number of defects. Our simulation shows that the corresponding value of L is 15 μm.

The propagation time delay ratio increases with the number of mono-vacancy defects and reaches 17.3 % when 6 defects are considered. Nevertheless, theoretical results show that SWCNT interconnects with 6 mono-vacancy defects would offer lower propagation time delays than ideal Cu interconnects when $L > 10$ μm [11]. The lower propagation time delay in SWCNTs has been attributed to their better conductivity – 40% larger than that of ideal bulk Cu – and their larger mean free path. If we consider the surface and grain boundary scattering of Cu, CNT interconnects will have a much better propagation time delay than Cu interconnects.

IV. CONCLUSIONS

Our statistical study shows that mono-vacancy defects induce significant fluctuations in SWCNT resistance. Interestingly, the obtained median values for resistance show an Ohmic-like behaviour depending only on SWCNTs diameter but not on their chirality. From these findings, we can derive an equation to describe the relationship between the diameter of SWCNT, the number of mono-vacancy defects, and the defective resistance. Our circuit simulation results also show that the propagation time delay ratio follows a similar pattern when the number of mono-vacancy defects in SWCNT increases. This indicates that SWCNT interconnects should be robust against variability issues related to their chirality if implemented in next generation CMOS circuits.

ACKNOWLEDGMENT

REFERENCES

[1] W. Wu, S. H. Brongersma, M. V. Hove and K. Maex, "Influence of sruface and grain-boundary scattering on the resisitvity", *Appl. Phys. Lett.,* vol. 84, no. 15, pp. 2838-2840, 2004.

[2] W. Steinhögl, G. Schindler, G. Steinlesberger, M. Traving, and M. Engelhardt, "Comprehensive study of the resistivity of copper wires with lateral dimensions of 100 nm and smaller", *J. Appl. Phys.,* vol. 97, 023706, 2005.

[3] A. Todri-Sanial, R. Ramos, H. Okuno, J. Dijon, A. Dhavamani, M. Wislicenus, K. Lilienthal, B. Uhlig, T. Sadi, V. P. Georigev, A. Asenov, S. M. Amoroso, A. R. Brown, A. Pender, C. Millar, F. Motzfeld, B. Gotsmann, J. Liang, G. Goncalves, N. Rupesinghe, and K. Teo, "A Survey of Carbon Nanotube Interconnects for Energy Efficient Integrated Circuits", *IEEE Circuits and Systems Magazine*, vol. 17, pp. 47-62, 2017.

[4] B. Q. Wei, R. Vajtai, and P. M. Ajayan, "Reliability and current carrying capacity of carbon nanotubes", *Appl. Phys. Lett.,* vol. 79, no. 8, pp. 1172-1174, 2001.

[5] S. Berber, Y. Kwon, and D. Tománek, "Unusually High Thermal Conductivity of Carbon Nanotubes", *Phys. Rev. Lett.*, vol. 84, 4613, 2000.

[6] H. Li, W. Liu, A. M. Cassell, F. Kreupl, and K. Banerjee, "Low-Resistivity Long-Length Horizontal Carbon Nanotube Bundles for Interconnect Applications—Part I: Process Development", *IEEE Trans. Electron Device*, vol. 60, no. 9, pp. 2862-2869, 2013.

[7] C. Subramaniam, T. Yamada, K. Kobashi, A. Sekiguchi, D. N. Futaba, M. Yumura and K. Hata, "One hundred fold increase in current carrying capacity in a carbon nanotube–copper composite", *Nat.Commun.* vol. 4, 2202, 2013.

[8] M. Bockrath, W. Liang, D. Bozovic, J. H. Hafner, C. M. Lieber, M. Tinkham and H. Park, "Resonant Electron Scattering by Defects in Single-Walled Carbon Nanotubes", *Science*, vol. 291, 283, 2001.

[9] Atomistix Tool Kit (2016.4), QuantumWise A/S

[10] Y. Hancock, K. Saloriutta, A. Uppstu, A. Harju, M. J. Puska, "Spin-Dependence in Asymmetric, V-Shaped-Notched Graphene Nanoribbons", *J. Low Temp. Phys.*, vol. 153, pp. 393-398, 2008.

[11] A. Naeemi and J. D. Meindl, "Compact Physical Models for Multiwall Carbon-Nanotube Interconnects", *IEEE Electron Device Lett.,* vol. 27, no. 5, pp. 338-340, 2006.